HHS Public Access

Author manuscript

Nature. Author manuscript; available in PMC 2015 July 29.

Published in final edited form as:

Nature. 2015 January 29; 517(7536): 621–625. doi:10.1038/nature14112.

Lineage-negative Progenitors Mobilize to Regenerate Lung Epithelium after Major Injury

Andrew E. Vaughan[1], **Alexis N. Brumwell**[1], **Ying Xi**[1], **Jeffrey Gotts**[1], **Doug G. Brownfield**[2], **Barbara Treutlein**[3], **Kevin Tan**[1], **Victor Tan**[1], **Fengchun Liu**[1], **Mark R. Looney**[1], **Michael Matthay**[1], **Jason R. Rock**[4], and **Harold A. Chapman**[1]

[1]Department of Medicine, Cardiovascular Research Institute, and Lung Biology Center, UCSF, San Francisco, California, 94143, USA

[2]Department of Biochemistry, Stanford University School of Medicine and Howard Hughes Medical Institute, Stanford, California 94305, USA

[3]Max Planck Institute for Evolutionary Anthropology, Department of Evolutionary Genetics, Deutscher Platz 6, 04103 Leipzig

[4]Department of Anatomy, School of Medicine, UCSF, San Francisco, California, 94143, USA

Abstract

Broadly, tissue regeneration is achieved in two ways: by proliferation of common differentiated cells and/or by deployment of specialized stem/progenitor cells. Which of these pathways applies is both organ and injury-specific[1–4]. Current paradigms in the lung posit that epithelial repair can be attributed to cells expressing mature lineage markers[5–8]. In contrast we here define the regenerative role of previously uncharacterized, rare lineage-negative epithelial stem/progenitor (LNEPs) cells present within normal distal lung. Quiescent LNEPs activate a ΔNp63/cytokeratin 5 (Krt5+) remodeling program after influenza or bleomycin injury. Activated cells proliferate and migrate widely to occupy heavily injured areas depleted of mature lineages, whereupon they differentiate toward mature epithelium. Lineage tracing revealed scant contribution of pre-existing mature epithelial cells in such repair, whereas orthotopic transplantation of LNEPs, isolated by a definitive surface profile identified through single cell sequencing, directly demonstrated the proliferative capacity and multipotency of this population. LNEPs require Notch signaling to

Correspondence and requests for materials should be addressed to A.V. (andrew.vaughan@ucsf.edu) or H.C. (hal.chapman@ucsf.edu).

Supplementary Information is linked to the online version of the paper at ww.nature.com/nature

Author Contributions. A.V. and H.C. designed the study, analyzed the data, and wrote the manuscript. A.V. performed lineage tracing, flow cytometry purification, and characterization of lung cells; J.G. titered PR8 virus and initiated all infections; A.B. isolated lung cell suspensions, assisted with flow cytometry, and designed and performed most of the immunostaining; Y.X. assisted with biochemistry, RNA analysis, and immunostaining; K.T. and V.T. managed the mouse genotyping and performed in vivo mouse experiments; V.T. isolated lung cells, designed quantification methods, and ; F.L. and M.L. performed lung transplantations; M.M. procured and screened human lungs; D.B. and B.T. synthesized libraries and provided initial data analysis for RNA-Seq experiments J.R. provided key reagents and assisted with study design.

FPKM files from single cell RNA-Seq experiments were deposited in Gene Expression Omnibus (GEO Accession # GSE61300).

The authors declare no competing financial interests.

Readers are welcome to comment on the online version of the paper.

activate the ΔNp63/Krt5+ program whereas subsequent Notch blockade promotes an alveolar cell fate. Persistent Notch signaling post-injury led to parenchymal micro-honeycombing, indicative of failed regeneration. Lungs from fibrosis patients show analogous honeycomb cysts with evidence of hyperactive Notch signaling. Our findings indicate distinct stem/progenitor cell pools repopulate injured tissue depending on the extent of injury, and the outcomes of regeneration or fibrosis may ride in part on the dynamics of LNEP Notch signaling.

Influenza infection challenges pulmonary regenerative capacity due to the widespread ablation of epithelial cells in substantial areas of lung (Extended Data Fig. 1G–H)[8]. A robust expansion of regenerative Krt5+ cells in the lung parenchyma following influenza infection has been observed in mice[8], which we confirmed (Extended Data Fig. 1). In addition we directly observed migration (Supplementary Videos) and identified coexpression of integrin α6β4 (Extended Data Fig. 1–2). These cells also appear variably after bleomycin injury, where ~1/3 of the Krt5+ cells resolved into type II pneumocytes by 50 days post-injury (Extended Data Fig. 3). A cellular origin and mechanistic framework for expansion after influenza, and potential parallels in human lung injury, remain unknown.

To define the cell-of-origin, we lineage traced mature cell types implicated in epithelial repair. Krt5+ cells appearing by day 11 post influenza infection were essentially completely untraced using CC10− or SPC-CreERT2 drivers (Fig. 1B–E, Extended Data Fig. 1I). Analysis at 7–8 days post-injury confirmed mutual exclusivity of CC10-Cre labeled cells and the Krt5+ cells (Fig. 1B). Conflicting results in other reports are likely caused by tamoxifen persistence (discussed online, Extended Data Fig. 4).

A small fraction (13%) of expanded Krt5+ cells bear the Krt5-CreERT2 lineage label (Fig. 1F–G), raising the possibility that tracheal basal cells might migrate distally during injury. We transplanted sections of fluorescent trachea into syngeneic animals and a non-fluorescent left lung into a fluorescent mouse[9]. Abundant Krt5+ cells arose after infection but none were fluorescent (Fig. 1H, Extended Data Fig. 1J–K). Upper-airway basal cells therefore do not contribute to this phenomenon and instead implicate a lineage-negative epithelial progenitor(s) (LNEP) as the major source of ΔNp63+/Krt5+ cells.

To characterize quiescent LNEPs we used β4 expression in CC10-CreERT2 mice to segregate LNEPs from club cells in uninjured lungs (Fig. 2A) and confirmed minimal expression of mature lineage markers (Extended Data Fig. 5C). The CC10− β4+ (LNEP containing) population uniquely expressed ΔNp63 (Extended Data Fig. 5C). ΔNp63+ cells were identified *in situ* scattered sporadically throughout distal airways (Fig. 2C). These cells did not express detectable Krt5 protein (Extended Data Fig. 5A). In a total of 65 small airways examined in two mice, we identified 24 ΔNp63+ cells. Only 7 of the 24 cells were labeled in Krt5-CreERT2 mice (Fig. 2C, Extended Data Fig. 5A), likely explaining the small fraction of post-injury Krt5+ cells bearing the Krt5-CreERT2 lineage label (Fig. 1F–G).

Given the infrequency of ΔNp63+ cells we suspected progenitor activity of the CC10− β4+ population might be restricted to a smaller subset. Immunostaining revealed multicilia in 78% of this population, whereas ΔNp63+ cells were less than 1% (Extended Data Fig. 5B). To address this heterogeneity, we performed single cell RNA-seq on CC10− β4+ cells and

rare Krt5-CreERT2-labeled cells, a subset of this population (Fig. 2I). ΔNp63 transcript was detected in several cells in the CC10− β4+ population (red ○, far left) as well as the Krt5-traced cells (green Δ) (Fig. 2B). ANOVA comparison between putative LNEPs (Krt5-traced cells combined with all p63-expressing cells) and the remaining cells revealed enrichment of ~900 genes (>2 fold change, >1 FPKM, $p \leq 0.05$) in the LNEP group (Supplementary File 1). We note enrichment for pluripotency-associated transcription factors (Myc, Klf4) in the LNEP group (Fig. 2C) while many genes enriched in the remaining cells (Fig. 2C top rows, Supplementary File 2) are known markers of ciliated cells[10]. Surprisingly, ΔNp63+ CC10− β4+ cells most closely related to the Krt5-traced cells also expressed cilia-associated genes (Fig. 2B, denoted by *). Cytospins of CC10− β4+ cells revealed primary cilia on ΔNp63+ cells and additional cells without discernible ΔNp63 (Fig 2D′), indicating the LNEP profile extends to a larger fraction of ΔNp63 low/neg cells.

To assess the potential of LNEPs *in vivo*, we devised a transplantation assay by which ~10^5 fluorescent CC10-β4+ cells were delivered orthotopically into influenza-injured mice (Fig. 2D). Seeded LNEPs developed into multicellular structures in two patterns seemingly dependent on location: areas of type II cells virtually indistinguishable from surrounding endogenous type II cells (Extended Data Fig 6A–B, H) and engraftments expressing Krt5 (Extended Data Fig. 6A,C) and CC10 (Extended Data Fig. 6G) near endogenous Krt5+/ CC10+ structures. β4- type II cells engrafted infrequently in small clusters (<8 cells), and expressed only alveolar markers (Extended Data Fig. 6I). CC10+ cells could engraft but exhibited scant differentiation, even losing CC10 expression (Extended Data Fig. 6J–K). Transplantation of multi-ciliated cells resulted in only occasional persistence of single cells without structures (Extended Data Fig. 6L), consistent with their lack of progenitor properties[11,12].

Transplantation of mixed eGFP and tdTomato-expressing LNEPs demonstrated engraftments to be largely non-overlapping (Fig. 2E) and highly proliferative (Extended Data Fig. 6E), arguing for near-clonal expansion. Although mature type II cells do not express integrin β4[13], clones derived from donor LNEPs exhibited β4/SPC co-expression 5 days after transplant (Extended Data Fig. 6E′), confirming their LNEP origin. These data demonstrate multipotency of LNEPs as well as the viability of orthotopic cell transplantation as a functional tool.

We interrogated the RNA-Seq analysis and identified enrichment for CD14 in ΔNp63+ CC10− β4+ cells (*, Fig. 2B). In combination with CD200, which further selects against multi-ciliated cells (Extended Data Fig. 5E), CD14+ cells were isolated and transplanted. β4+ CD200+ CD14+ cells (~3000) (Fig. 2F) phenocopied the larger (150,000) CC10-β4+ population (Fig. 2G–H, Extended Data Fig. 7A–C), validating this small population as the active LNEPs. Utilizing a complementary approach, distal Krt5-CreERT2-labeled ΔNp63+ cells within the LNEP fraction were transplanted (1000 cells per mouse) (Fig. 2I). Multipotency was again observed, though we noted many fewer SPC expressing cells (Fig. 2J–K, Extended Data Fig. 7D–E). We posit that isolation using Krt5-driven Cre enriches for LNEPs that have undergone partial commitment to the Krt5 program, whereas surface marker-based selection represents a less biased approach. This is consistent with lineage

analysis (Fig. 1H) indicating Krt5-CreERT2-traced cells can only account for a small fraction of the Krt5+ expansion.

Accordingly, LNEPs cultured *ex vivo* did not express Krt5 even when treated with various trophic/morphogenic factors (Supplementary Table 2). However, bronchoalveolar lavage fluid (BALF) from injured mice induced dramatic proliferation and Krt5 expression. 77 ± 13% of colonies treated with the BALF stained positive for Krt5 (Fig. 3A–D) whereas type II cells treated with the same BALF did not respond.

Although the active principle(s) in injury BALF is uncertain, a screen of pathway inhibitors implicated a critical role of Notch. The γ-secretase inhibitor DAPT in conjunction with active BALF attenuated intensity and Krt5+ colony fraction (22.7 ± 13%) (Fig. 3C–D). This prompted us to analyze Notch activity *in vivo*. Notch1 ICD and the canonical Notch target gene Hes1 were evident in the nucleus of parenchymal Krt5+ cells post-influenza (Fig. 3E–F). Notch activity was further validated using a Notch reporter mouse (Cp-eGFP) (Extended Data Fig. 8A–B). When DAPT was administered to mice post-influenza, the fraction of lung area bearing Krt5+ cells by day 11 was markedly reduced (Fig. 3G, Extended Data Fig. 7H).

During development Notch signaling is known to suppress alveolar differentiation in both the lung and mammary gland[14,15]. When LNEPs were cultured in the presence of γ-secretase inhibitors we observed strong induction of SPC expression, further promoted by IBMX[16] (Fig. 3H–I). Therefore, persistent Notch signaling prevents alveolar differentiation whereas removal of this signal promotes maturation toward type II cells. This result proved relevant to the long-term outcome of regeneration in the influenza injury model.

Although regions of relatively normal histology bearing the Krt5-CreERT2 trace develop after resolution of bleomycin injury (Extended Data Fig. 3E), we were surprised to find few traced SPC+ type II cells after influenza (Extended Data Fig. 8E). Instead, large regions of Krt5-Cre traced epithelial cysts were present in all mice examined between day 52 and day 200 post-injury (n=7 mice) (Fig. 4A). These cysts consisted of CC10+ cells, scattered Krt5+ cells, otherwise nondescript epithelial cells, but very few SPC+ cells (Fig. 4A, Extended Data Fig. 8C–E), raising the possibility of ongoing Notch activity in cystic epithelium. Strong Hes1 expression persisted in Krt5-CreER traced cysts cells indefinitely (Fig. 4B, Extended Data Fig. 8F) whereas it is normally undetectable in alveolar epithelium (Extended Data Fig. 8G). The same correlation was observed in transplant experiments: LNEP-derived Krt5+ & CC10+ areas exhibited strong Hes1 whereas it was low or absent in areas of type II cell differentiation (Extended Data Fig. 6B–D). Notch antagonism *in vivo* via intranasal delivery of DBZ (in conjunction with dexamethasone and IBMX) resulted in a significant increase in the number of cyst-derived SPC+ cells (12.3% vs 1.6%) (Fig. 3J–L).

Persistent cysts bear a strong resemblance to “micro-honeycombing” in lungs of Idiopathic Pulmonary Fibrosis (IPF) patients (Fig. 4C–D). These lungs (n=10) showed almost all cystic epithelia were comprised of Krt5+ cells surrounded by either additional metaplastic Krt5+ cells or pseudostratified epithelium with ectopic but otherwise typical basal cells[17]. Distinct foci of hyperplastic SPC+ cells were also present. Notch activity correlated with Krt5+ cysts

but was absent in most hyperplastic SPC+ cells (Fig. 4D–F and Extended Data Fig. 9A–D) and in normal alveolar regions (Extended Data Fig. 9K).

In lungs from scleroderma patients (n = 7) fibrotic areas displayed the IPF pattern of persistent Krt5+/Hes1+ cystic structures (Extended Data Fig. 9E,G–H). However, in 3 less fibrotic specimens, we observed extensive Krt5/SPC double positive cells lining alveoli (Fig. 4G, Extended Data Fig. 9F). Although the origin of this Krt5+ expansion is uncertain in humans, we note ΔNp63+/Krt5− cells in normal terminal airways (Extended Data Fig. 9I), analogous to LNEPs in mice.

These experiments identify a rare, undifferentiated epithelial population that is the major responder in distal lung following severe damage (Extended Data Fig. 10A). Notch signaling modulates the quiescence, activation, and differentiation state of murine LNEPs (Extended Data Fig. 10B), providing a signaling paradigm to frame the dynamic aspects of LNEP function. The persistently abnormal parenchymal structures that derive from LNEPs following influenza infection represent a failed regenerative process, promoted at least in part by ongoing Notch activity. The striking parallels to the currently inexplicable micro-honeycombing that characterizes progressive fibrotic lung disease, including hyperactive Notch, suggest inappropriate Notch signaling may also be a major contributor to failed regeneration in chronic lung disease.

Methods

Animals

SPC-CreERT2 (**Sftpc$^{tm1(cre/ERT2,rtTA)Hap}$**), Krt5-CreERT2 (**Krt5$^{tm1.1(cre/ERT2)Blh}$**), CC10-CreERT2 (**Scgb1a1$^{tm1(cre/ERT)Blh}$**), FoxJ1-CreERT2 (**Tg$^{(Foxj1-cre/ERT2)1Blh}$**, and Cp-eGFP (**Tg(Cp-EGFP)25Gaia**) mice are previously described. [13,18–20] All of these strains were bred to either mTmG (**Gt(ROSA)26Sor$^{tm4(ACTB-tdTomato,-EGFP)Luo}$**)[21] or Ai14-tdTomato (**Gt(ROSA)26Sor$^{tm14(CAG-tdTomato)Hze}$**)[22] mice in order to generate mice expressing a fluorophore in Cre-expressing cells. SPC-CreERT2, Krt5-CreERT2 and CC10-CreERT2 mice were developed in a 129 background and backcrossed to C57BL6 for at least 3 generations. For transplant experiments, mTmg and/or Ub-GFP (**Tg(UBC-GFP)30Scha**)[23] were used for donor cells. For all experiments, 6–8 week old animals of both sexes were used in equal proportions. Investigators were not blinded to mouse identity. All studies were approved by UCSF IACUC, protocol AN088356-03. All animal studies utilized a minimum of 3 mice per group with the exception of DBZ (see below).

For lineage analysis for the cell of origin of Krt5+ cells, mice were administered three doses (Krt5-CreERT2) or five doses (SPC-CreERT2 and CC10-CreERT2) of 0.25 mg/g body weight tamoxifen in 50 ul corn oil. A chase period >21 days was employed to insure the absence of residual tamoxifen prior to injury.

Injury (Influenza, Bleomycin)

Mice were administered 280 FFU of Influenza A/H1N1/Puerto Rico/8/34 (PR8) intra-nasally. PR8 virus dissolved in 30 μl of PBS was pipetted onto the nostrils of heavily anesthetized mice (visual confirmation of agonal breathing), whereupon mice aspirated the

fluid directly into their lungs. The mice were allowed to recover and weighed twice a week. For experiments analyzing the lineage fate of Krt5+ cells, a single dose of 0.125 mg/g body weight tamoxifen was administered at day 10 post-PR8 infection.

Infective viral particles were assayed by inoculation of either stock virus or homogenate (in 1 ml PBS) of left lung, spleen, and brain onto 96 well plates of confluent MDCK cells. After one hour, samples were decanted and replaced with serum-free media containing TPCK trypsin at 100 μg/ml. Fifteen hours later, the cells were fixed in 100% methanol, and then underwent indirect immunocytochemistry using Millipore mouse anti-influenza A (MAB 8257) at 1.25 μg/ml, followed by Vector® 102 biotinylated horse anti-mouse, and the biotin/avidin system (PK-4002) with diaminobenzidine as a chromogen. Samples were processed in triplicate over dilutions, and foci were counted in wells that yielded 30–100 discrete foci.

1.7 U/kg body weight bleomycin was administered intra-tracheally. Mice were weighed twice a week. For lineage tracing Krt5+ cells post-bleomycin, a single dose of 0.125 mg/g body weight tamoxifen was administered at day 17 post-bleomycin.

Treatment of animals with γ-secretase inhibitors

For DAPT administration, mice received 50 mg/kg body weight DAPT in 20 ul DMSO per intraperitoneal injection, for the indicated periods. For intranasal DBZ administration, 30 μmoles/kg body weight DBZ was suspended in 50 ul sterile PBS and sonicated in a Bioruptor UCD-200 for 15 min total, 30 sec intervals on ice. In DBZ experiments, both DBZ and vehicle group also received 2.5 μg/g body weight dexamethasone (Sigma) in the intranasal solution and 10 mg/kg 3-Isobutyl-1-methylxanthine (IBMX, Sigma) i.p. daily. Both DAPT and DBZ were obtained from Toronto Research Chemicals. >7500 Krt5-CreERT2-labeled cells were quantified for SPC expression in at least 2 individual lobes from each mouse.

Orthotopic lung transplantation

Left lung transplants were carried out using the method described by Okazaki and colleagues.[24] The donor animal was anesthetized and injected with heparin (50 units) immediately prior to perfusion of the lung vasculature with 5 ml of ice cold Perfadex solution (Xvivo Perfusion, Goteborg Sweden), clamping of the hilar structures, and removal from the donor animal. The left lung was transplanted into the recipient animal using the cuff anastomosis technique.

Orthotopic tracheal transplantation

The donor animal was anesthetized and with the aid of microscopic dissection, a segment of trachea composed of 5–7 tracheal rings was removed. The recipient animal was anesthetized and the donor trachea was interposed using proximal and distal anastomoses[9].

Immunofluorescence analysis of tissue

After euthanasia, lungs were either immediately inflated with OCT and flash frozen or inflated with 4% PFA and fixed for 1 hour at room temperature and subsequently embedded in OCT. 7 um sections were cut on a cryostat, with fresh frozen tissue immediately fixed for

5 min in 4% paraformaldehyde at room temperature. All sections were subsequently incubated for 3 × 10 minute intervals with 1 mg/ml sodium borohydride (Sigma) in PBS to reduce aldehyde-induced background fluorescence. Slides were subsequently blocked ≥ 1 hour in PBS + 1% bovine serum albumin (Affymetrix), 5% nonimmune horse serum (UCSF Cell Culture Facility), 0.1% Triton X-100 (Sigma), and 0.02% sodium azide (Sigma). Slides were incubated overnight in primary antibodies listed below, diluted in block solution. Slides were washed three times with PBS + 0.1% Tween 20, and incubated with secondary antibodies (typically Alexa Fluor conjugates, Life Sciences) at a 1:2000 dilution ≥ 1 hour. Finally, slides were again washed, incubated with 1 uM DAPI for 5 min, and mounted using Prolong Gold (Life Sciences).

The following antibodies were used: rabbit anti-proSPC (1:3000; Millipore, AB3786), goat anti-proSPC (1:2000; Santa Cruz, M-20), goat anti-CC10 (1:10,000, a gift from Barry Stripp), rabbit anti-Krt5 (1:1000; Covance, PRB-160P), chicken anti-Krt5 (1:1000; Covance, SIG-3475), rabbit anti-ΔNp63 (1:100; Biolegend, POLY6190), rat anti-CD45 (1:200, BD 30-F11), sheep anti-eGFP (1:500; Pierce, 10396164), rabbit anti-phospho histone H3 (1:500; Millipore, 06-570), rabbit anti-Hes1 (1:1000; Cell Signaling, D6P2U), rabbit anti-activated Notch1 (1:1000; Abcam, ab8925), mouse anti-acetylated tubulin (1:500, Sigma, 6-11B-1).

Quantification of lineage tracing

Samples were prepared for immunofluorescence staining. Quantification at day 11 post-influenza is the result of counting >2900 cells (CC10 trace), >4000 cells from (SPC trace), or >1300 (Krt5 trace) from at least 3 mice per genotype. Cells were counted from >5 sections per mouse and included at least 3 individual lobes. Mutual exclusivity of CC10-traced and Krt5+ cells at day 7–8 was determined with a smaller sample size, n=2 mice, 12 Krt5+ airways/>500 cells examined. Only mice possessing the appropriate genotype were used in studies.

Epithelial cell isolation and flow cytometry

Lung epithelial cells were isolated as previously described[13], with the following modifications. After installation with agarose and subsequent hardening by a brief incubation on ice, each lobe was cut away from the mainstem bronchi. The proximal-most ¼ of each lobe surrounding the bronchi was then cut away to minimize the inclusion of basal cells in the cell preparation, and the previous protocol was followed from this point on.

For FACS analysis, single cell preparations were incubated 30–45 minutes at 4°C with the following primary antibodies: PE, Alexa Fluor 488, or BV421-conjugated rat anti-mouse EpCAM (1:500; Biolegend, G8.8), Alexa Fluor 647 or PE-conjugated rat anti-mouse integrin β4 (1:75; BD, 450-9D), Alexa 647-conjugated CD200 (1:100, Biolegend, OX-90), and PE/Cy7 conjugated CD14 (1:100, Biolegend, Sa14-2). Antibody incubations were done in DMEM (without phenol red) + 2% FBS and cells were washed twice with PBS after antibody incubations. Sorting and analysis was performed on BD FACS Aria cytometers.

Orthotopic cell transplantation

Recipient C57BL/6 mice were infected with PR8 (see **Animals**). At 9 days post-infection, donor cells were sorted from mTmG or Ub-GFP mice (**Animals**) and resuspended in 50ul sterile PBS. Recipient mice received cell solution intranasally as described above for influenza administration. The total number of β4+ cells ranged from 150,000 to 350,000 per transplant (n=6), and equivalent numbers of β4- cells were always transplanted into injured littermates for comparison. For transplantation of Krt5-CreERT2-labeled cells, 1000 cells were transplanted per recipient (n = 2). For β4+ CD14+ CD200+ cell transplants, 3000–10,000 cells were transplanted per mouse (n=3). FoxJ1-CreERT2 or CC10-CreERT2-labeled cell transplanted were performed in n=3 or 4 mice each ($1–3 \times 10^5$ cells per mouse). Endpoint analysis was performed at day 21 post-infection unless otherwise noted. For analysis of proliferation, recipient mice were administered 50 mg/kg body weight Edu (Santa Cruz) in PBS daily. Edu was detected with Click-iT® EdU Alexa Fluor® 488 Imaging Kit (Invitrogen).

Primary cell culture

Isolated primary lung epithelial cells were plated and cultured on Matrigel as follows. 8-well chamber slides were coated with 150 ul Matrigel per well, allowed to solidify at 37°, and then equilibrated SABM (Lonza) for at least 30 minutes prior to cell plating. 15 to 40,000 cells were plated in each well of and maintained in “baseline” media consisting of SAGM (Lonza) supplemented with 5% charcoal-stripped FBS and 10 ng/ml KGF (FGF-7, Peprotech). Other growth factors were included in the media only when indicated and are summarized in Supplementary Table 2.

Bronchioalveolar lavage fluid (BALF) was harvested from injured animals for cell culture as follows. Euthanized mice were intratracheally intubated prior to cardiac perfusion and 1 ml of baseline media was lavaged. The lungs were repeatedly lavaged with the media at least three times. BALF was then centrifuged three times for 5 min spins at 1500xG to remove the cells and other debris. Clarified BALF was finally filtered through a 0.25 um Spin-X filter (Sigma) to remove any additional debris and to ensure a cell-free preparation. BALF prepared in this way was either added to cells immediately or frozen in aliquots at −80° C and was added to cultured cells without dilution.

Long term cell culture

Cells isolated as above were maintained in SAGM as above, with the addition of 10 uM Y-27632 (Sigma) and 50 ng/ml murine noggin (Peprotech). Cells were passaged every 7–10 days by initial incubation with 25 U/ml Dispase at 37° for 20 minute to liberate colonies. Single cell dissociation was performed by additional 10 minute incubation with 2 mM EDTA in PBS in combination with mechanical disaggregation by pipetting.

γ-secretase treatment of LNEPs *in vitro*

LNEPs maintained as above were dissociated and re-plated directly into SAGM baseline media with added DAPT or GSI-X (Calbiochem) at 40 or 20 μM concentrations (unless

otherwise indicated). For SPC induction experiments, IBMX was added when indicated. LNEPs were cultured for 7–10 days and then analyzed by immunofluorescent staining.

Immunofluorescence analysis of cultured cells

Cells grown on matrigel were fixed 5–10 minutes in IHC Zinc Fixative (BD) and subsequently stained as indicated above, except that all staining solutions were prepared with TBS as the zinc fixative reacts with phosphate.

Live slice imaging

Krt5-CreERT2/tdTomato mice were administered 280 FFU PR8 (as above) and received a single 0.25 mg/kg dose of tamoxifen 24 hours prior to sacrifice at the indicated time points. Injured mice were euthanized and perfused and lavaged with PBS. Lungs were instilled with 2% low-melting point agarose and ~300 um slices were prepared on a vibratome. Lung slices were maintained in SAGM + 10 ng/ml KGF during imaging with the addition of 500 nM hydroxytamoxifen (Sigma) in order to induce recombination in all Krt5-expressing cells. Slices were imaged continuously for 12 hours in a 37° C chamber on an inverted stage with a Leica SP5 confocal microscope. Images obtained were deconvoluted with Bitplane Imaris for presentation.

Quantitative reverse transcriptase PCR

RNA was isolated from sorted cells using the Promega RNA Reliprep kit. cDNA was synthesized and amplified using the Ovation PicoSL WTA V2 kit (NuGen). RT-PCR reactions were performed using Faststart Universal SYBR green Master Mix (Roche) and run on an Eppendorf Realplex^2 thermocycler. Primer sequences are as listed:

SPC	ATGGACATGAGTAGCAAAGAGGT	CACGATGAGAAGGCGTTTGAG
CC10	ATGAAGATCGCCATCACAATCAC	GGATGCCACATAACCAGACTCT
Keratin 5	TCCAGTGTGTCCTTCCGAAGT	TGCCTCCGCCAGAACTGTA
ΔNp63	ATGTTGTACCTGGAAAACAATGCC	CAGGCATGGCACGGATAAC
Jagged1	CCTCGGGTCAGTTTGAGCTG	CCTTGAGGCACACTTTGAAGTA
Jagged2	CAATGACACCACTCCAGATGAG	GGCCAAAGAAGTCGTTGCG
Hey1	GCGCGGACGAGAATGGAAAA	TCAGGTGATCCACAGTCATCTG
Aqp5	AGAAGGAGGTGTGTTCAGTTGC	GCCAGAGTAATGGCCGGAT
ABCA3	GCTTGAAGATCCAGTCGGAGA	CATAGCGAATGTAGTCCTCGAAG
CGRP	GCGGGCTCTAGCTTGGACAG	AAGGTGTGAAACTTGTTGAGGT
Sox2	GCGGAGTGGAAACTTTTGTTC	GGGAAGCGTGTACTTATCCTTCT
Foxj1	CATCTACAAGTGGATCACGGAC	GAGCAGGCGCTCTGCGTACTG

Single Cell RNA-seq

Distal lung epithelial cells were isolated and FACS sorted as described above from CC10-CreERT2/mTmG mice. In addition, tdTomato+ cells were sorted from tamoxifen-treated Krt5-CreERT2/tdTomato mice. Sorted single cells were captured on a medium-sized (10–

17_μm cell diameter) microfluidic RNA-seq chip (Fluidigm) using the Fluidigm C1 system. All downstream steps (lysis, cDNA synthesis/amplification, library preparation, sequencing, and raw data processing) were performed exactly as previously described.[10] FPKM files for each cell were analyzed using Fluidigm Singular® software running in R.

Human tissues

All human tissue samples were obtained from UCSF Interstitial Lung Disease Blood and Tissue Repository and are classified as Non-identifiable Otherwise Discarded Human Tissues.

Statistics

For calculations involving single cell RNA-seq, Fluidigm Singular® software running in R was used. All other statistical calculations were performed using Graphpad Prism. P values were calculated from two-tailed t-tests (paired or unpaired depending on experimental design) or ANOVA for multivariate comparisons. Variance was analyzed at the time of t-test analysis. This data is not included in the manuscript but is available upon request.

Extended Data

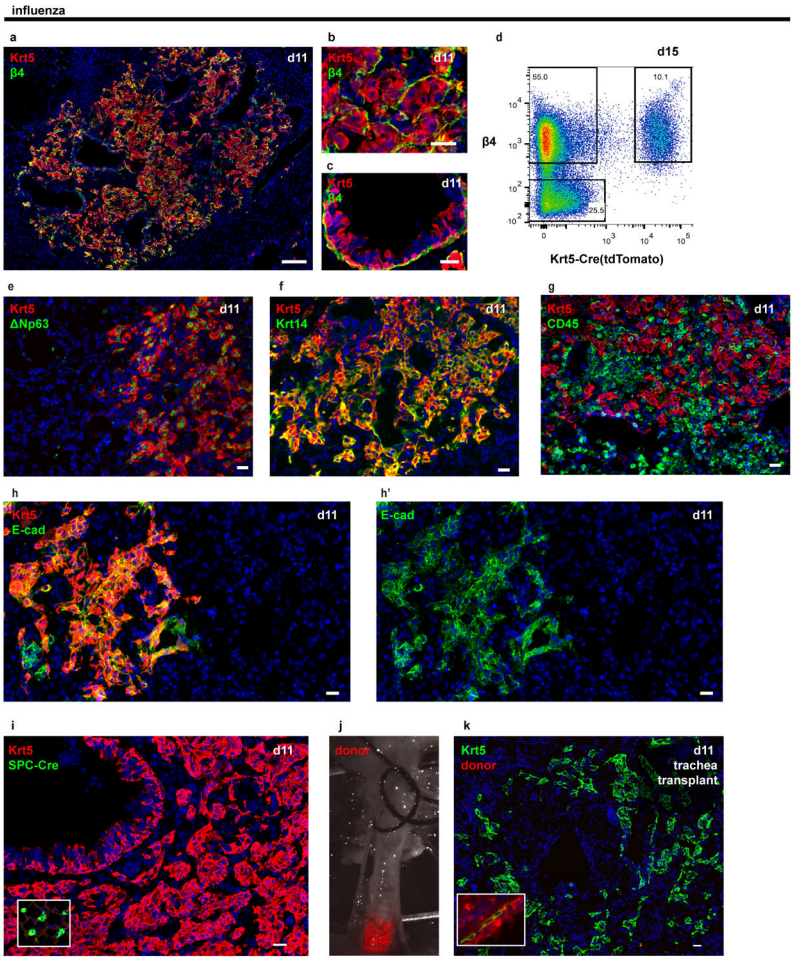

Extended Data Figure 1. Characterization of influenza-induced Krt5+ cells

a–c, Airway (**c**) and alveolar (**a–b**) Krt5+ cells strongly express β4 after influenza injury. **d**, FACS plot of epithelial (EpCam+) cells from tamoxifen-treated Krt5-CreERT2/tdTomato mice at day 15 post-influenza, demonstrating β4 expression in nearly all traced (tdTomato+) cells. **e–f**, Most Krt5+ cells co-express ΔNp63 (**e**) and Krt14 (**f**). **g–h**, Expanded Krt5+ cells are invariably associated with abundant CD45+ inflammatory cells (**g**) and few if any remaining normal E-cadherin+ epithelial cells other than the Krt5+ cells themselves (**h**). **i**, Krt5+ cells are unlabeled in SPC-CreERT2/mTmG mice. Inset in (**i)** demonstrates appropriate labeling of type II cells in an uninjured region of the same lung. **j–k,** Krt5+ cells are not fluorescent after trachea transplantation from tdTomato donor. Basal cells in transplanted section of trachea retained fluorescence (**j**, inset in **k**). Scale bars = 100 μm in **a** and 20 μm in all others.

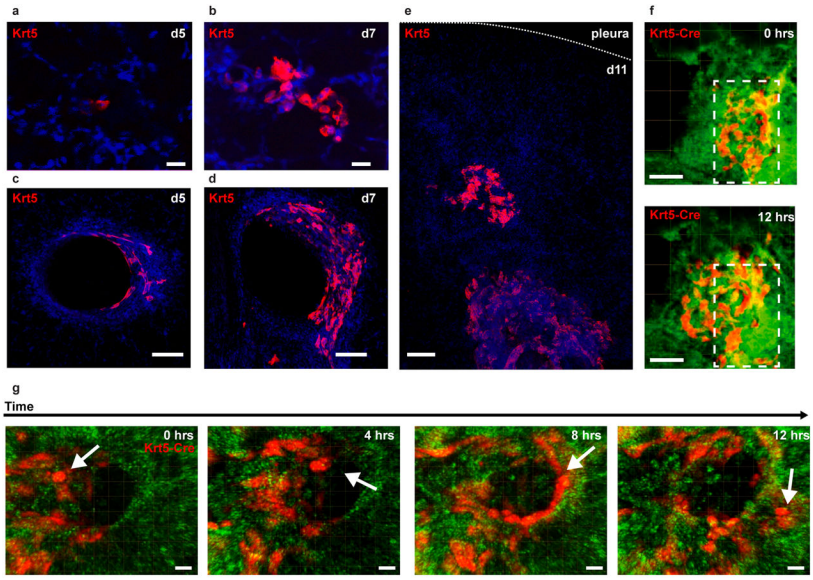

Extended Data Figure 2. Influenza-induced Krt5+ cells arise in both airways and alveoli and migrate across, around, and through airway and parenchymal tissue

a–b, Krt5+ cells are detected in alveoli as early as day 5 and are found in larger clusters over time. **c–d**, Krt5+ cells similarly arise in airways in greater abundance with time. **e**, Distinct alveolar and airway expansion is apparent 11 days after infection. **f**, Freeze-frames of live imaging from a Krt5-CreERT2/tdTomato mouse 11 days post-influenza, wherein tdTomato+ cells migrate from their original location (white box) outward. See Supplementary Video 1a. **g**, Freeze-frames from a small airway in the same mouse; arrow denotes a single cell crossing the basement membrane. See Supplementary Video 2. Scale bars = 20 μm in **a–b** and **g**, 100 μm in all other panels.

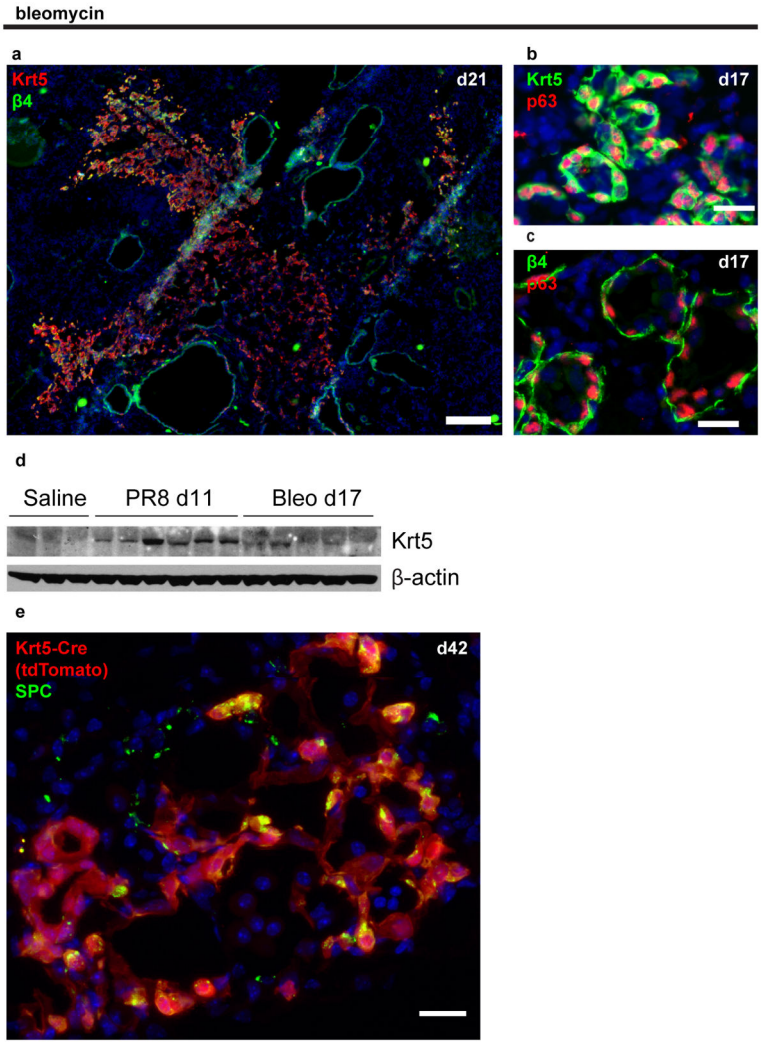

Extended Data Figure 3. Characterization of bleomycin-induced Krt5+ cells

a–c, β4+ Krt5+ cells also arise after bleomycin injury and express ΔNp63 (**b–c**). **d**, Western blotting demonstrating more pronounced and reproducible Krt5 induction after influenza injury than bleomycin at day 11 or 17, respectively. Each lane was loaded with whole lung lysate from a single mouse; average % lung area corresponding to a band in influenza-injured mice is 3.6 ± 0.5% (n=13 mice quantified, see Fig. 3G as an example). **e**, Lineage tracing of bleomycin-injured Krt5-CreERT2 mice reveal traced (tdTomato+) type II cells expressing SPC and cells morphologically resembling type I cells. 31% of Krt5-Cre traced cells express SPC by day 50 post-bleomycin (n=3 mice, 264 Krt5-CreERT2-labeled cells counted). Scale bars = 100 μm in **a** and 20 μm in all others. Full scan of western blot in **d** is available as Supplementary Figure 1.

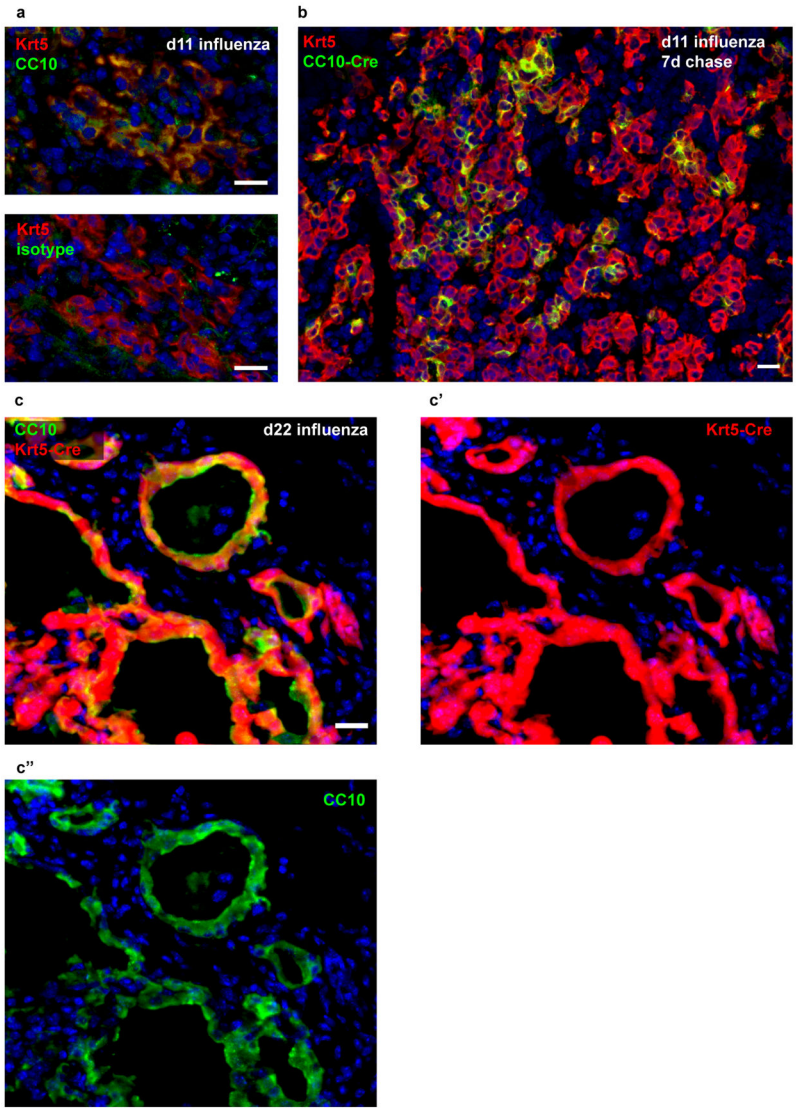

Extended Data Figure 4. Krt5+ cells do not arise from CC10-expressing progenitors but rather upregulate CC10 during expansion

a, Krt5+ cells express detectable levels of CC10 (top) compared to isotype control (bottom) in alveolar clusters (**a**). **b**, Representative image of CC10-CreERT2 lineage trace wherein waiting only 7 days after tamoxifen administration prior to influenza injury results in significant labeling of Krt5+ cells (quantified in Figure 1D). **c**, Strong CC10 expression in Krt5-CreERT2 traced (tdTomato+) cells by day 22 post-influenza. For comparison see single channel images (**c′ and c″)** of the same region. Scale bars = 20 μm.

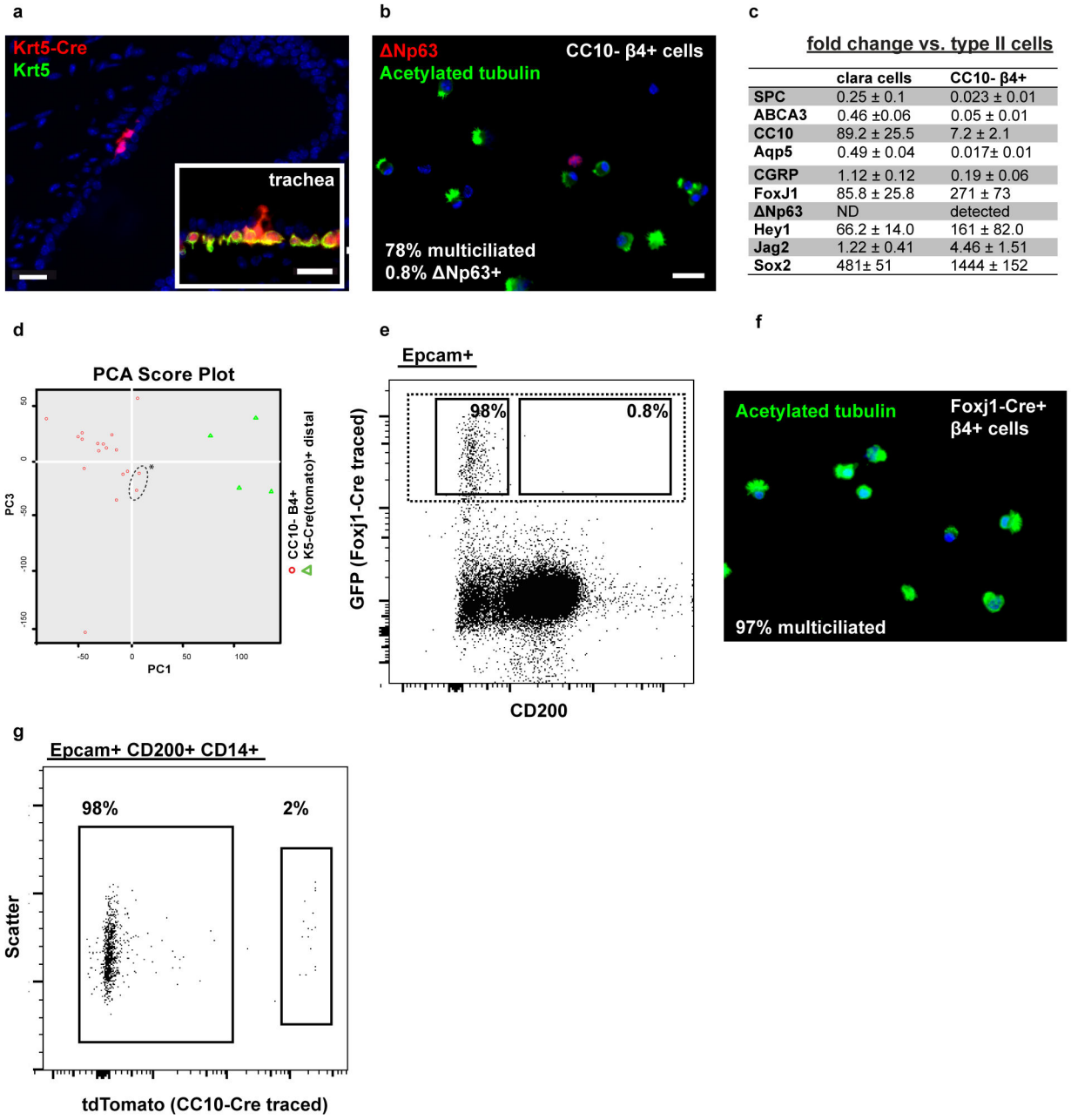

	clara cells	CC10- β4+
SPC	0.25 ± 0.1	0.023 ± 0.01
ABCA3	0.46 ±0.06	0.05 ± 0.01
CC10	89.2 ± 25.5	7.2 ± 2.1
Aqp5	0.49 ± 0.04	0.017± 0.01
CGRP	1.12 ± 0.12	0.19 ± 0.06
FoxJ1	85.8 ± 25.8	271 ± 73
ΔNp63	ND	detected
Hey1	66.2 ± 14.0	161 ± 82.0
Jag2	1.22 ± 0.41	4.46 ± 1.51
Sox2	481± 51	1444 ± 152

Extended Data Figure 5. Heterogeneity of the LNEP-containing CC10− β4+ population

a, Rare Krt5-CreERT2 traced (tdTomato+) cells were observed in uninjured distal lung airways that lacked Krt5 staining compared to trachea basal cells (inset) in the same section. All distal tdTomato+ cells express ΔNp63 but most ΔNp63+ cells are untraced (see Fig. 2C). **b**, Cytospins of sorted CC10− β4+ cells reveal the presence of abundant multiciliated cells (green, acetylated tubulin+) and a small fraction of ΔNp63+ cells (red). **c**, qRT-PCR analysis of mature lineage genes and genes of interest in all populations. n= 3 biological replicates, Mean ± S.D. **d**, PCA plot of cells sequenced in Fig. 2B, demonstrating that p63+ cells in the CC10− β4+ population (outlined, *) cluster with multi-ciliated cells. **e**, CD200 is not

expressed by FoxJ1-CreERT2-labeled multi-ciliated cells, highlighting its use in excluding such cells. **f**, Cytospin of Foxj1-CreERT2-labeled β4+ cells demonstrating faithful selection for multi-ciliated cells (198 cells quantified). **g**, Gating on CD14 expression within the Epcam+ β4+ CD200+ population excludes CC10-expressing club cells. Scale bars = 20 μm.

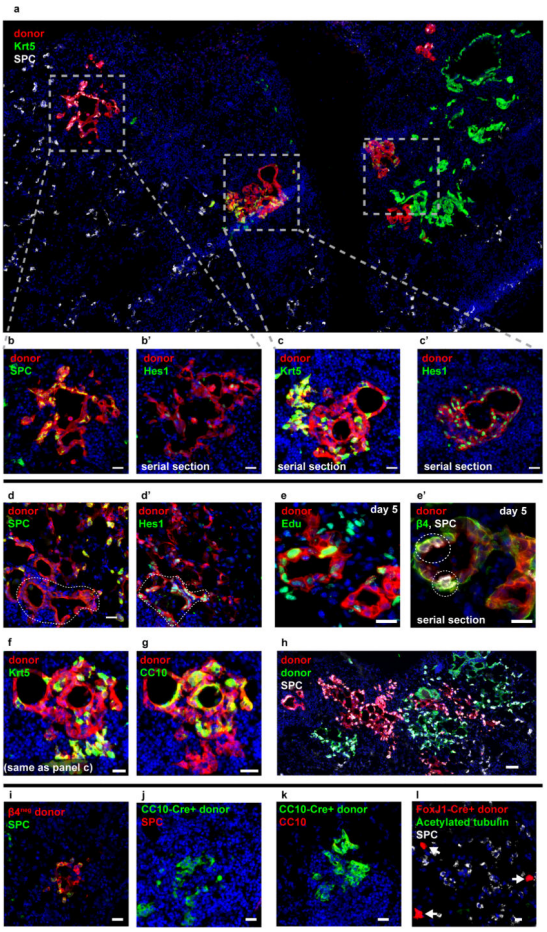

Extended Data Figure 6. Orthotopic transplantation of LNEPs reveals their multipotency and differentiation appropriate to the local microenvironment

a, Several distinct areas of LNEP engraftment (red) reflect differentiation in response to location. Left dashed box demonstrates SPC expression in engrafted cells with nearby endogenous SPC-expressing cells (white); far right dashed box demonstrates Krt5 expression in engrafted cells and nearby endogenous Krt5-expressing cells (green). **b–c**, Cells in regions of SPC+ differentiation (**b**) lack Hes1 expression (**b′**), while those in areas of Krt5+ differentiation (**c**) strongly express Hes1 (**c′**). **d**, Distinct areas of LNEP engraftment demonstrate an inverse relationship between SPC expression (**d**) and Hes1 expression (**d′**) in probable single clones. **e,** Examination of transplanted cells 5 days after engraftment demonstrate abundant Edu incorporation (see Methods) indicative of proliferation. At this time point cells can be identified co-expressing β4 and SPC (**e′, circled**). **f–g**, Krt5+ cells and CC10+ cells were often found clustered in single regions of engraftment. **h**, Many engrafted cells in Fig. 2E are also SPC positive. **i**, β4- type II cells engraft in small clusters and only express SPC. **j–k**, CC10+ cells engraft but do not express

SPC, CC10, or Krt5. **l**, Multi-ciliated cells engraft but only persist as isolated single cells, losing acetylated tubulin expression. Scale bars = 100 μm in **a** and 20 μm in all other panels.

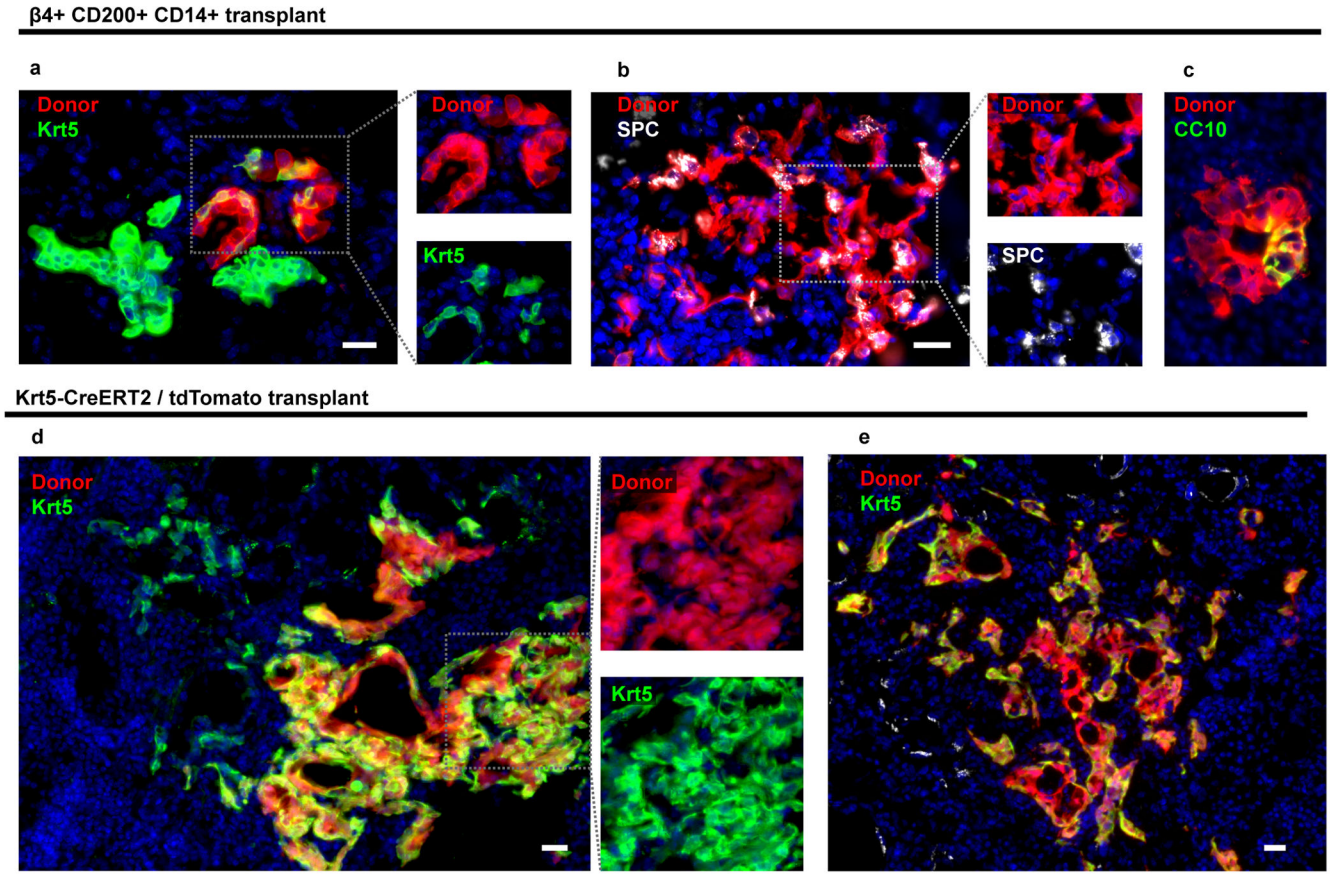

Extended Data Figure 7. Transplantation of β4+ CD14+ CD200+ and Krt5-CreERT2-traced cells recapitulates multipotency of the heterogenous CC10− β4+ population

a, Single channels images from Fig. 2H demonstrate Krt5 expression in transplanted β4+ CD14+ CD200+ cells. **b–c**, Transplanted β4+ CD14+ CD200+ can also differentiate towards type II cells (**b**) and club cells (**c**). **d–e**, Transplantation of rare Krt5-CreERT2-traced cells from uninjured mice resulting in donor-derived Krt5+ cell expansion indistinguishable from endogenous expansion. **d–e** are representative images from 4 attempted transplants, two of which exhibited engraftment in 2 or 4 individual lobes. Scale bars = 20 μm in all panels.

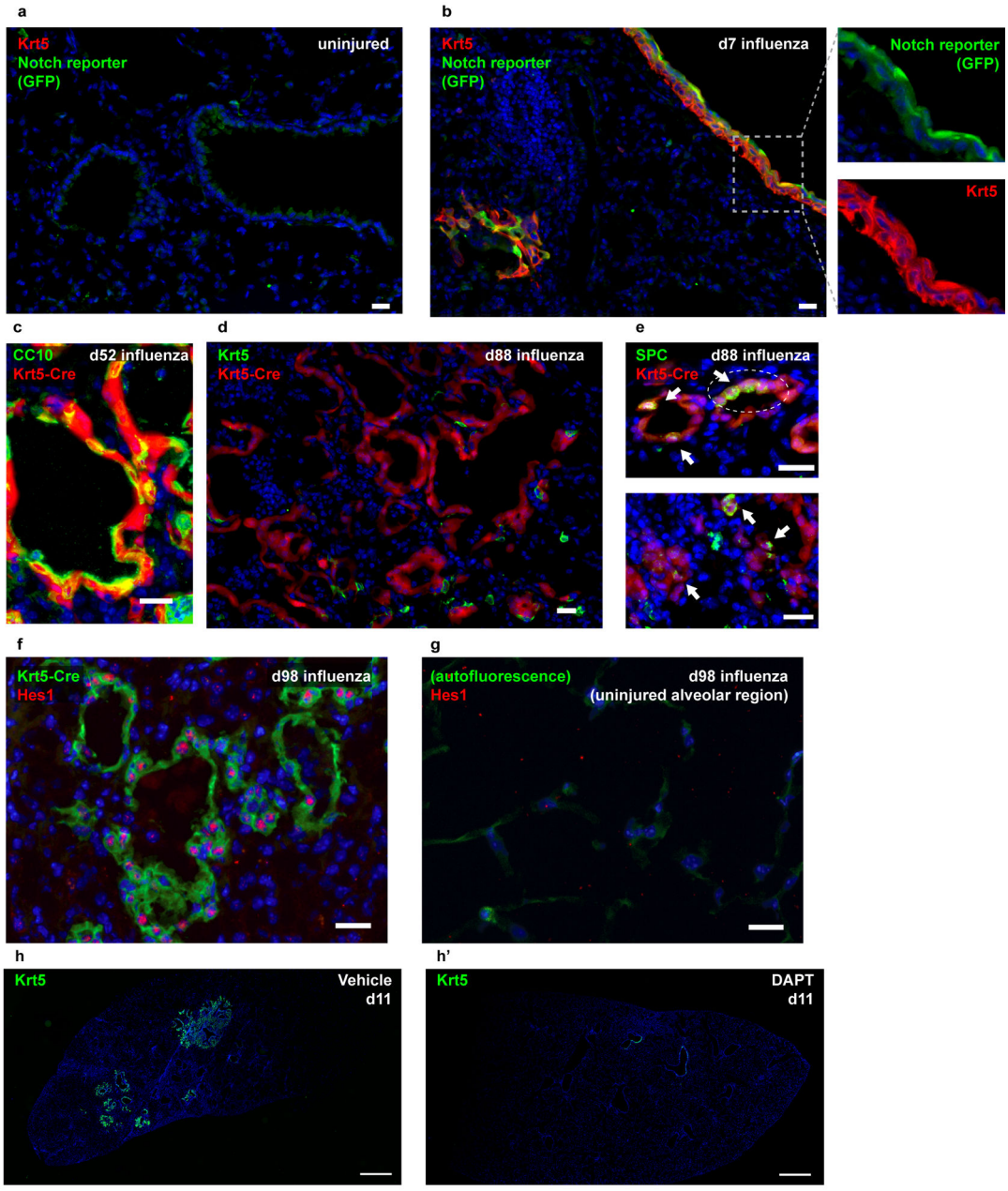

Extended Data Figure 8. Notch activity in normal and injured lung

a, Uninjured Notch reporter mice (Cp-eGFP) show dim GFP in small airways and no detectable GFP in alveoli. **b**, Krt5+ cells arising in distal airways express GFP in Notch reporter mice 7 days after influenza infection. **c–d**, Some Krt5+ cells persist within Krt5-CreERT2 labeled (tdTomato+) cysts (**d**) long-term after influenza injury, while many traced cells express CC10 (**c**). **e**, Cysts rarely contain SPC+ type II cells (**a′, arrows**). **f–g**, Hes1 expression is maintained in Krt5-CreERT2 traced (GFP+) cysts cells 98 days post-influenza (**f**) but is absent in normal alveolar parenchyma from the same mice g). **h**, Representative images of Krt5+ cell expansion in vehicle (**h**) or DAPT (**h′**) treated mice at day 11 post-influenza, quantified in Fig. 3G. Scale bars = 20 μm in **ag** and 100 μm in **h**.

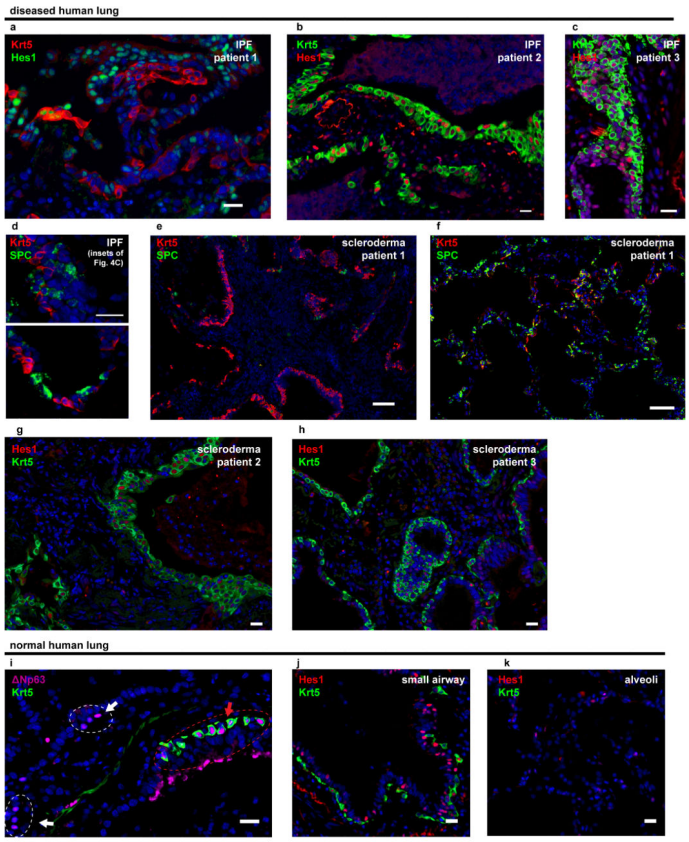

Extended Data Figure 9. IPF and scleroderma lungs both contain Hes1+ honeycomb cysts, but scleroderma lungs also possess SPC/Krt5 co-expressing cells. Normal human lungs contain putative LNEPs and lack Hes1 in alveoli

a–**d**, Honeycomb cysts in several IPF lungs; many Krt5+ cells as well as surrounding cystic epithelium demonstrate strong nuclear Hes1 signal. **e**, Region of scleroderma honeycombing similar to IPF lung. **f**, Scleroderma subpleural alveolar region with type II cell hyperplasia demonstrating cells co-expressing SPC and Krt5. **g**–**h,** Cystic epithelium in scleroderma lungs expresses Hes1 as in IPF. **i**, Krt5- ΔNp63+ cells (white outlines) distinct from Krt5+ ΔNp63+ basal cells (red outlines) are present in distal airways. **j**–**k**, Hes1 staining is apparent in small airways of normal lung (**j**) but very low in alveolar parenchyma (**k**). All images are from patient samples in addition to those shown in Fig. 4. Scale bars = 100 μm in **e**–**f** and 20 μm in all otherss.

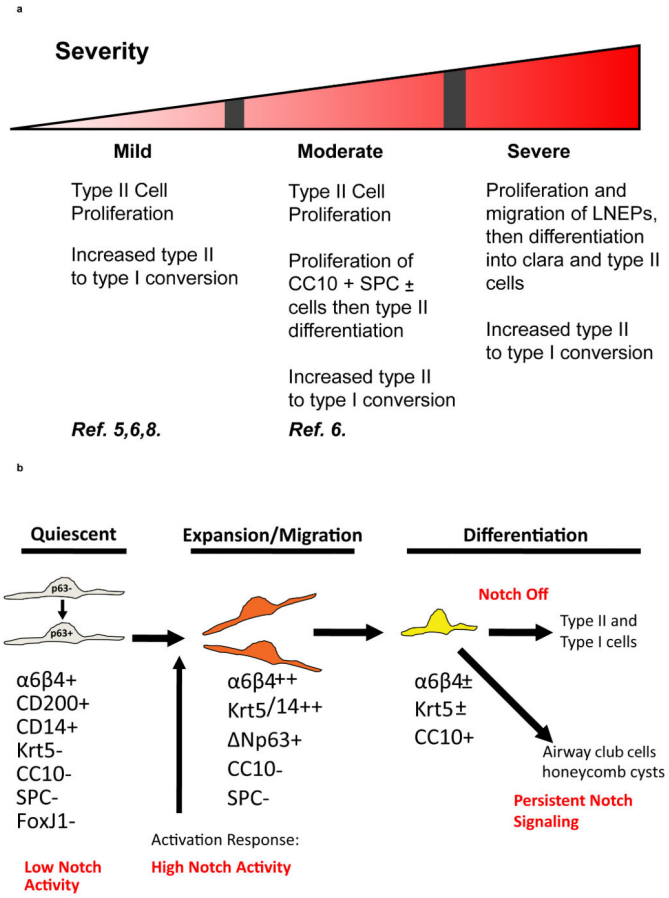

Extended Data Figure 10. Hierarchical cellular responses to injury severity and Notch-regulated LNEP dynamics

a, Distinct epithelial cell types contribute to regeneration depending on the severity of parenchymal injury. Examples of each are referenced. **b**, Notch signaling regulates the activation, expansion, and differentiation of LNEPs. Notch is required for activation and maintenance of LNEPs. Alveolar differentiation requires subsequent loss of Notch activity, while persistent Notch results in either airway differentiation or abnormal cystic honeycombing.

Supplementary Material

Refer to Web version on PubMed Central for supplementary material.

Acknowledgments

This work was supported by NIH grants RO1 HL44712, UO1 HL111054, and a sponsored research agreement with Daiichi Pharmaceuticals. A.V is supported by F32 HL117600-01. The authors thank Thomas Kim for assistance with animal work and thank Kaitlin Corbin for assistance with Imaris software. Mouse line art was created by Ashley van de Wiel. We also thank Paul Wolters at the UCSF Interstitial Lung Disease Blood and Tissue Repository for procuring diseased lung tissues. We thank the Nina Ireland Program for Lung Health that supported the tracheal/lung transplant experiments.

References

1. Clevers H. The Intestinal Crypt, A Prototype Stem Cell Compartment. Cell. 2013; 154:274–284. [PubMed: 23870119]
2. Gurtner GC, Werner S, Barrandon Y, Longaker MT. Wound repair and regeneration. Nature. 2008; 453:314–321. [PubMed: 18480812]
3. Tanimizu N, Mitaka T. Re-evaluation of liver stem/progenitor cells. Organogenesis. 2014; 10:0–1.
4. King RS, Newmark PA. The cell biology of regeneration. The Journal of Cell Biology. 2012; 196:553–562. [PubMed: 22391035]
5. Desai TJ, Brownfield DG, Krasnow MA. Alveolar progenitor and stem cells in lung development, renewal and cancer. Nature. 2014; 507:190–194. [PubMed: 24499815]
6. Barkauskas CE, et al. Type 2 alveolar cells are stem cells in adult lung. J Clin Invest. 2013; 123:3025–3036. [PubMed: 23921127]
7. Giangreco A, et al. Stem cells are dispensable for lung homeostasis but restore airways after injury. Proc Natl Acad Sci USA. 2009; 106:9286–9291. [PubMed: 19478060]
8. Kumar PA, et al. Distal airway stem cells yield alveoli in vitro and during lung regeneration following H1N1 influenza infection. Cell. 2011; 147:525–538. [PubMed: 22036562]
9. Schrepfer S, et al. Experimental orthotopic tracheal transplantation: The Stanford technique. Microsurgery. 2007; 27:187–189. [PubMed: 17326196]
10. Treutlein B, et al. Reconstructing lineage hierarchies of the distal lung epithelium using single-cell RNA-seq. Nature. 2014; 509:371–375. [PubMed: 24739965]
11. Rawlins EL, Ostrowski LE, Randell SH, Hogan BLM. Lung development and repair: Contribution of the ciliated lineage. Proc Natl Acad Sci USA. 2007; 104:410–417. [PubMed: 17194755]
12. Rawlins EL, Hogan BL. Ciliated epithelial cell lifespan in the mouse trachea and lung. Am J Physiol Lung Cell Mol Physiol. 2008; 295:L231–234. [PubMed: 18487354]
13. Chapman HA, et al. Integrin α6β4 identifies an adult distal lung epithelial population with regenerative potential in mice. J Clin Invest. 2011; 121:2855–2862. [PubMed: 21701069]
14. Guseh JS, et al. Notch signaling promotes airway mucous metaplasia and inhibits alveolar development. Development. 2009; 136:1751–1759. [PubMed: 19369400]
15. Chakrabarti R, et al. Elf5 Regulates Mammary Gland Stem/Progenitor Cell Fate by Influencing Notch Signaling. STEM CELLS. 2012; 30:1496–1508. [PubMed: 22523003]
16. Wang J, et al. Differentiated human alveolar epithelial cells and reversibility of their phenotype in vitro. Am J Respir Cell Mol Biol. 2007; 36:661–668. [PubMed: 17255555]
17. Seibold MA, et al. The Idiopathic Pulmonary Fibrosis Honeycomb Cyst Contains A Mucocilary Pseudostratified Epithelium. PLoS ONE. 2013; 8:e58658. [PubMed: 23527003]
18. Van Keymeulen A, et al. Distinct stem cells contribute to mammary gland development and maintenance. Nature. 2011; 479:189–193. [PubMed: 21983963]
19. Rawlins EL, et al. The Role of Scgb1a1+ Clara Cells in the Long-Term Maintenance and Repair of Lung Airway, but Not Alveolar, Epithelium. Cell Stem Cell. 2009; 4:525–534. [PubMed: 19497281]
20. Duncan AW, et al. Integration of Notch and Wnt signaling in hematopoietic stem cell maintenance. Nat Immunol. 2005; 6:314–322. [PubMed: 15665828]
21. Muzumdar MD, Tasic B, Miyamichi K, Li L, Luo L. A global double-fluorescent Cre reporter mouse. Genesis. 2007; 45:593–605. [PubMed: 17868096]
22. Madisen L, et al. A robust and high-throughput Cre reporting and characterization system for the whole mouse brain. Nat Neurosci. 2010; 13:133–140. [PubMed: 20023653]
23. Schaefer BC, Schaefer ML, Kappler JW, Marrack P, Kedl RM. Observation of Antigen-Dependent CD8+ T-Cell/Dendritic Cell Interactions in Vivo. Cellular Immunology. 2001; 214:110–122. [PubMed: 12088410]
24. Krupnick AS, et al. Orthotopic mouse lung transplantation as experimental methodology to study transplant and tumor biology. Nature protocols. 2009; 4:86–93. [PubMed: 19131960]

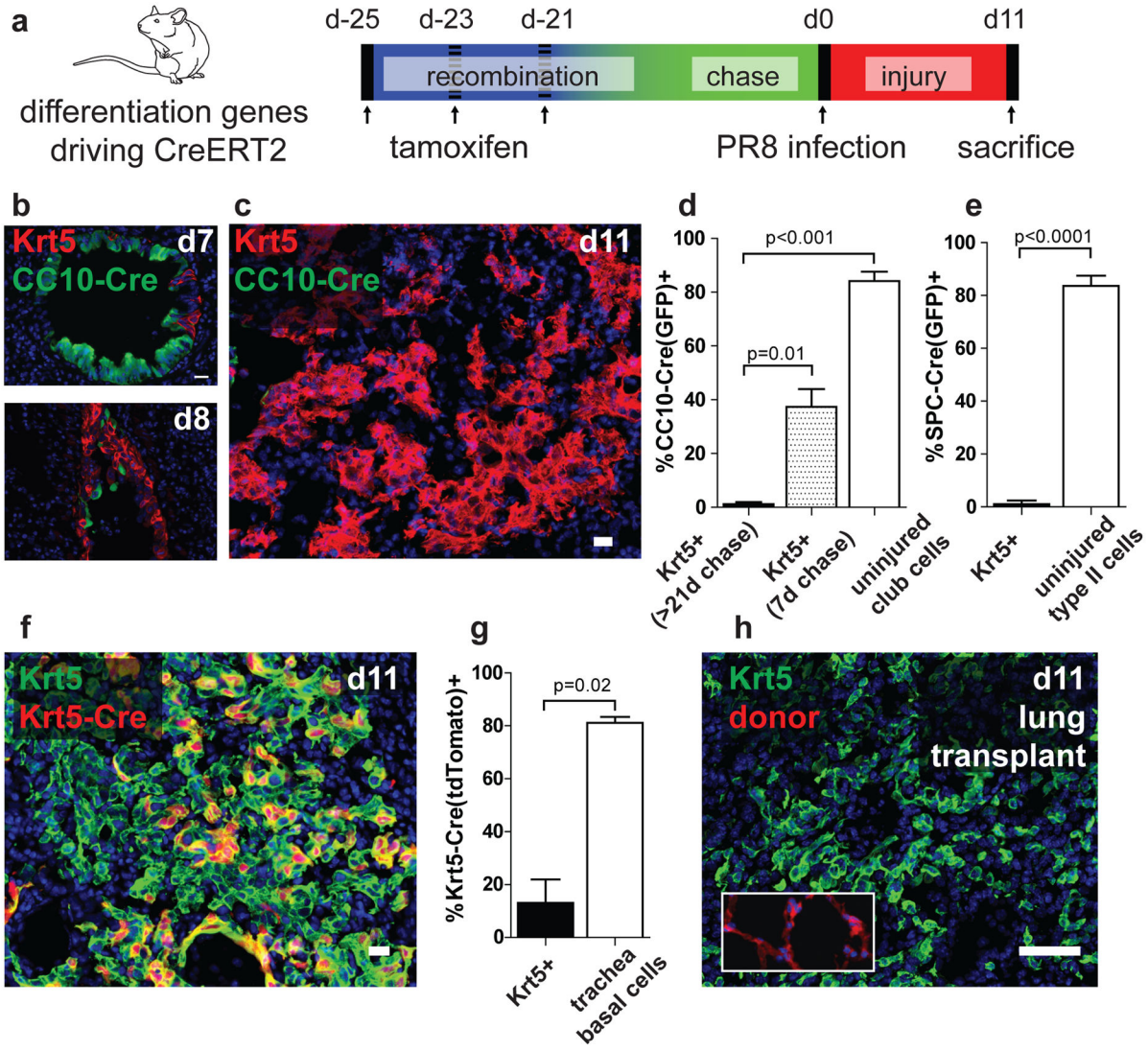

Figure 1. Injury-induced Krt5+ cells are derived from a lineage-negative precursor

a. Schematic depicting lineage analysis methodology. **b–c.** Krt5+ cells are untraced (GFP negative) after influenza injury in CC10-CreERT2/mTmG mice. **d–e.** Quantification of CC10 and SPC lineage tracing, expressed as percentage of cells counted bearing the respective lineage tag (see Methods). Short chase time after tamoxifen administration to CC10-CreERT2 mice results in significant trace in Krt5+ cells (**e**) (Supplemental Discussion). Means ± S.D., n=7 CC10-CreERT2 and n=3 SPC-CreERT2 mice quantified. **f–g,** A small fraction of Krt5+ cells bear Krt5-Cre trace (tdTomato+), quantified in (**g**) (n=3 Krt5-CreERT2 mice) **h**, Krt5+ cells are not fluorescent after lung transplantation from a wild-type donor into a tdTomato recipient. Non-transplanted lung tissue retained fluorescence (inset). Image representative of n=1 lung transplant. Scale bars = 20 μm. Source data available online.

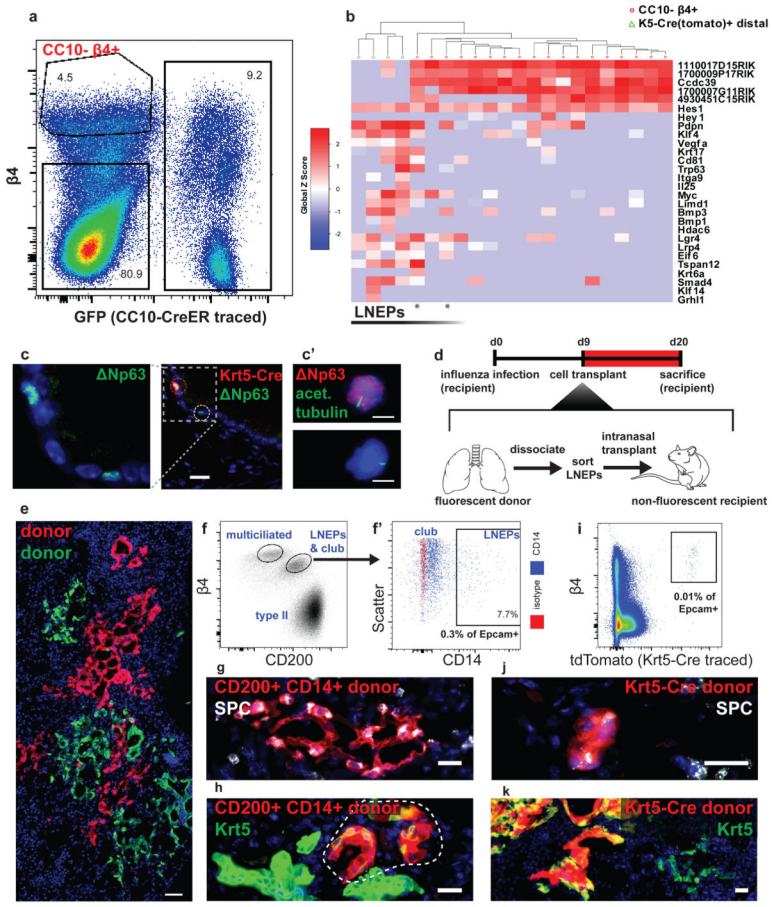

Figure 2. Isolation and transplantation of a lineage-negative distal epithelial population

a, FACS segregation of epithelial (EpCam+) cells by β4 expression and a CC10-CreERT2 lineage tag (GFP), demonstrating a β4+ population distinct from club cells. **b**, Hierarchical clustering/heat map of RNA-seq transcriptomes from single CC10− β4+ cells (○) and distal Krt5-CreERT2 traced cells (Δ) (columns). Listed genes (rows) were selected from >1200 differentially expressed genes identified by ANOVA. **c**, Immunofluorescent staining for ΔNp63 in uninjured lungs from Krt5-CreERT2/tdTomato mice. Single cells from cytospins of the CC10− β4+ population demonstrate primary cilium (green) in a subset of non-multiciliated cells (**c′**). **d**, Schematic depicting orthotopic cell transplantation methodology. **e**, Transplantation of LNEPs combined from eGFP or tdTomato-expressing donors into a single recipient. Most engrafted regions are exclusively GFP+ (green) or tdTomato+ (red) suggesting clonal expansion. **f–h,** FACS isolation and transplantation of β4+ CD200+ CD14+ LNEPs (**f**). Transplanted cells differentiate into both SPC+ (**g**) and Krt5+ (**h**) cells, representative of n=3 transplants. **i**, FACS isolation and transplantation of Krt5-CreERT2-labeled LNEPS also differentiate into SPC+ (**j**) and Krt5+ (**k**) cells, representative of n=2 transplants. Scale bars = 20 μm except **c′**=10 μm and **e** = 100 μm.

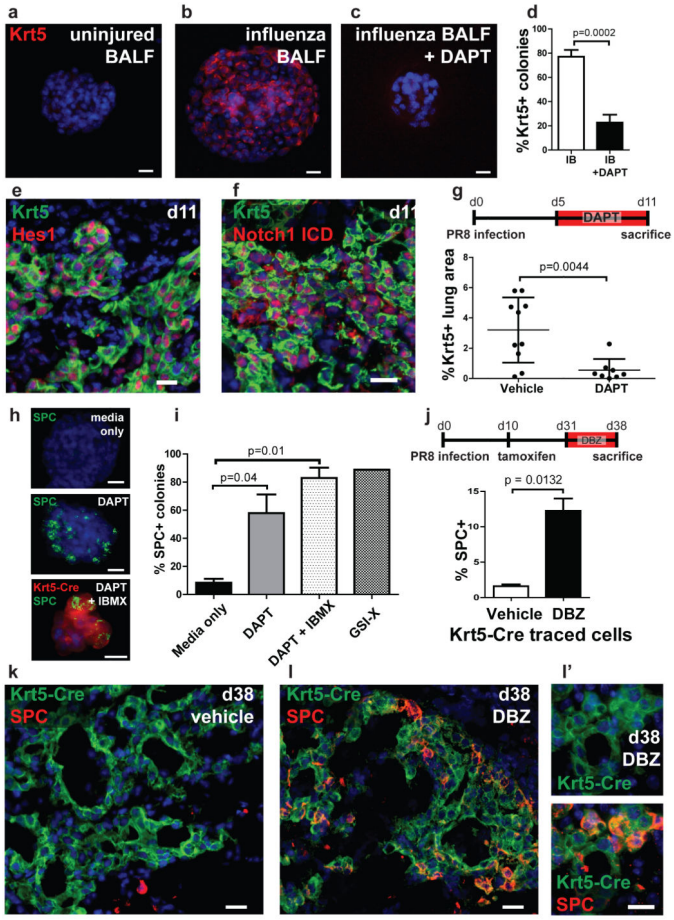

Figure 3. Activation and Krt5 expression by lineage-negative progenitors is Notch-dependent

a–c, LNEP colonies upregulate Krt5 only upon stimulation with BALF from influenza-injured mice (**b**) (n=6 experiments), a process blocked by γ-secretase inhibition (**c**) (n=4 experiments), quantified in (**d**). **e–f**, Hes1 (**e**) and Notch1 intracellular domain (**f**) are present in the nucleus of Krt5+ cells at day 11 indicating Notch activity. **g**, γ-secretase inhibition during influenza injury reduces Krt5+ cell activation/expansion as measured by fraction of lung section area; each dot = one section, two sections per mouse, n=5 (vehicle) or 4 (DAPT) mice per group. **h–i**, γ-secretase inhibition induces SPC expression in LNEPs *in vitro*, quantified in (**i**) (n=3 experiments). **h,** bottom panel, Krt5-CreERT2 lineage label could be observed in SPC+ cells after DAPT treatment *in vitro*. **j–l**, Representative images of Notch inhibition *in vivo* via intranasal administration of DBZ results in a significant increase in Krt5-CreERT2-traced SPC+ cells (**l**) versus labeled cells in vehicle-treated mice (**k**) post-influenza, quantified in (**j**) (n= 2 mice/group, >900 cells quantified per mouse in 2 sections from 2 separate lobes). IB = “influenza BALF”. Scale bars = 20 μm. Means ± S.D. Source data for (**g**) and (**j**) available online.

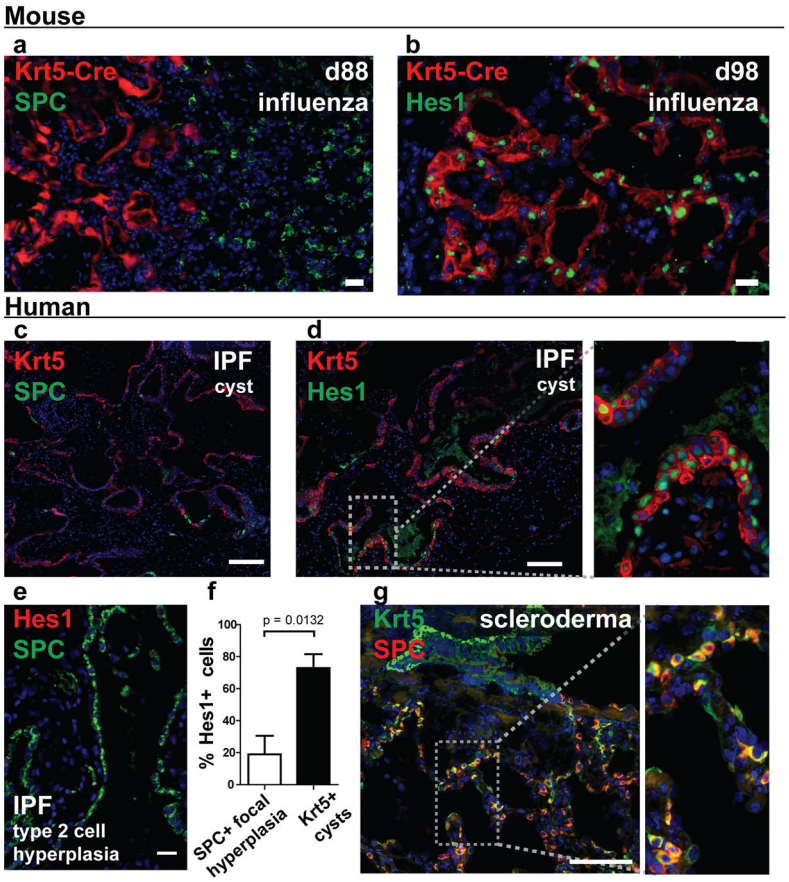

Figure 4. Persistent Notch activity promotes cystic honeycombing in both mouse and human

a, Krt5-CreERT2-traced (tdTomato+) cells develop into cystic structures at late time points post-influenza. **b**, Cyst cells demonstrate nuclear expression of Hes1 indicative of persistent Notch signaling. **c,** Lung from IPF patient bearing honeycomb cysts with mutually exclusive Krt5+ and SPC+ cells. **d**, IPF honeycomb cysts with nuclear Hes1 in Krt5+ cells and surrounding epithelium, similar to mouse (**b**). **e**, SPC+ type II cells in hyperplastic foci infrequently express Hes1, quantified in (**f**) (n=8 patients, means ± S.D). **g**, Scleroderma lung demonstrating sub-pleural Krt5+ and SPC+ cell expansion with many Krt5+/SPC+ double positive cells (**right**). Scale bars = 20 μm except **c** where scale bar = 100 μm.